Basal lamina strengthens cell membrane integrity via the laminin G domain-binding motif of α-dystroglycan

Renzhi Han[a], Motoi Kanagawa[a], Takako Yoshida-Moriguchi[a], Erik P. Rader[a], Rainer A. Ng[b], Daniel E. Michele[a], David E. Muirhead[c], Stefan Kunz[d], Steven A. Moore[e], Susan T. Iannaccone[f], Katsuya Miyake[g], Paul L. McNeil[h], Ulrike Mayer[i], Michael B. A. Oldstone[d,j], John A. Faulkner[b,k], and Kevin P. Campbell[a,1]

[a]Howard Hughes Medical Institute, Departments of Molecular Physiology and Biophysics, Neurology, Internal Medicine, and [e]Pathology, Roy J. and Lucille A. Carver College of Medicine, The University of Iowa, Iowa City, IA 52242; Departments of [b]Molecular and Integrative Physiology and [k]Biomedical Engineering, University of Michigan, Ann Arbor, MI 48109-0622; [c]Texas Scottish Rite Hospital for Children, Dallas, TX 75219; Departments of [d]Neuropharmacology and [j]Infectiology, The Scripps Research Institute, La Jolla, CA 92037; [f]Department of Pediatric Neurology, Children's Medical Center, University of Texas Southwestern Medical Center, Dallas, TX 75390; [h]Department of Cellular Biology and Anatomy, [g]Institute of Molecular Medicine and Genetics, The Medical College of Georgia, Augusta, GA 30912; and [i]Wellcome Trust Centre for Cell-Matrix Research, University of Manchester, Manchester M13 9PT, United Kingdom

This contribution is part of the special series of Inaugural Articles by members of the National Academy of Sciences elected in 2004.

Contributed by Kevin P. Campbell, June 12, 2009 (sent for review May 12, 2009)

Skeletal muscle basal lamina is linked to the sarcolemma through transmembrane receptors, including integrins and dystroglycan. The function of dystroglycan relies critically on posttranslational glycosylation, a common target shared by a genetically heterogeneous group of muscular dystrophies characterized by α-dystroglycan hypoglycosylation. Here we show that both dystroglycan and integrin α7 contribute to force-production of muscles, but that only disruption of dystroglycan causes detachment of the basal lamina from the sarcolemma and renders muscle prone to contraction-induced injury. These phenotypes of dystroglycan-null muscles are recapitulated by *Large*^{myd} muscles, which have an intact dystrophin–glycoprotein complex and lack only the laminin globular domain-binding motif on α-dystroglycan. Compromised sarcolemmal integrity is directly shown in *Large*^{myd} muscles and similarly in normal muscles when arenaviruses compete with matrix proteins for binding α-dystroglycan. These data provide direct mechanistic insight into how the dystroglycan-linked basal lamina contributes to the maintenance of sarcolemmal integrity and protects muscles from damage.

dystroglycanopathy | glycosylation | integrin | membrane damage | muscular dystrophy

The muscular dystrophies are genetically and clinically diverse (1, 2). Although great progress has been made in identification of genes responsible for various muscular dystrophies, we still do not have a mechanistic understanding of the function of these gene products and their roles in the pathogenesis of disease. One reason for this lack of understanding is that primary genetic alterations often lead to secondary changes, thereby triggering multiple pathogenic pathways. Compromised integrity of the sarcolemma has been proposed as the underlying mechanism for muscular dystrophy since 1852 (3); however, the molecular basis for this mechanism has never been clearly established.

The sarcolemma of each individual skeletal muscle fiber is closely associated with an extracellular protein matrix layer: the basement membrane (4–6). This membrane comprises both an internal felt-like basal lamina and an external reticular lamina composed of at least 10 secretory proteins that include members of the laminin family, perlecan, agrin, and the collagens (7, 8). The native basement membrane has a very substantial mechanical strength (5). Genetic mutations or deletions of some of these basement membrane proteins lead to a variety of defects, including early embryonic lethality and congenital muscular dystrophy. The basal lamina is linked directly to the cell membrane through transmembrane receptors including dystroglycan (DG) and the integrins, all of which bind laminin with high affinity (9, 10). In addition, DG also binds to many other basal lamina proteins containing laminin globular (LG) domains such as perlecan (11) and agrin (12). The functional role of the DG- and integrin-linked basal lamina in adult skeletal muscle physiology has not been fully investigated.

DG consists of a highly glycosylated, extracellular alpha subunit (α-DG) and a transmembrane beta subunit (β-DG), both of which are encoded by the gene *Dag1* and generated by posttranslational cleavage and processing (13). The matrix-binding capacity of α-DG depends on its extensive posttranslational glycosylation (14, 15), and this has emerged as a convergent target for a group of limb-girdle and congenital muscular dystrophies termed "secondary dystroglycanopathies". These include Fukuyama congenital muscular dystrophy, muscle-eye-brain disease, Walker–Warburg syndrome, congenital muscular dystrophy 1C (MDC1C) and 1D (MDC1D), as well as a milder form of limb-girdle muscular dystrophy, type 2I. Moreover, some pathogens target properly processed α-DG for cellular entry, including *Mycobacterium leprae*, Lassa fever virus (LFV), and lymphocytic choriomeningitis virus (LCMV) (16, 17). The early lethality in DG-null mice (18), the prevalence of diseases involving α-DG hypoglycosylation, and the coopting of normal α-DG for cellular entry by pathogens all support the hypothesis that DG-linked basal lamina plays an essential role in cell biology.

α7β1 integrin is predominantly expressed in adult skeletal muscle (10, 19). Mice lacking α7 integrin develop a mild form of muscular dystrophy (20) and mutations in the human integrin α7 gene have been found in a rare form of congenital muscular dystrophy (21). These observations suggest that the α7β1 inte-

Author contributions: R.H., M.K., and K.P.C. designed research; R.H., M.K., T.Y.-M., E.P.R., R.A.N., D.E. Michele, D.E. Muirhead, and J.A.F. performed research; S.K., S.A.M., S.T.I., K.M., P.L.M., U.M., and M.B.A.O. contributed new reagents/analytic tools; R.H., M.K., T.Y.-M., E.P.R., R.A.N., D.E. Michele, D.E. Muirhead, J.A.F., and K.P.C. analyzed data; and R.H., M.K., and K.P.C. wrote the paper.

The authors declare no conflict of interest.

Freely available online through the PNAS open access option.

[1]To whom correspondence should be sent at: Howard Hughes Medical Institute, Department of Molecular Physiology and Biophysics, The University of Iowa Carver College of Medicine, 4283 Carver Biomedical Research Building, 285 Newton Road, Iowa City, IA 52242-1101. E-mail: kevin-campbell@uiowa.edu.

This article contains supporting information online at www.pnas.org/cgi/content/full/0906545106/DCSupplemental.

grin complex is also important for normal skeletal muscle function. Different from α-DG binding to many basal lamina proteins, α7β1 has only been reported to bind laminin (10).

Here we report that despite both DG and integrin α7 contributing to the force-production of skeletal muscles, only the disruption of DG causes detachment of the basal lamina from the sarcolemma and renders the muscle prone to contraction-induced injury. More specifically, disruption of the LG domain-binding motif on α-DG is sufficient to induce these phenotypes. By using an assay that involves in situ membrane damage, we now demonstrate that sarcolemmal integrity is compromised in *Large*^{myd} muscles and in normal muscles when the UV-inactivated LCMV competes for association with α-DG. Therefore, our data suggest that the basal lamina strengthens sarcolemmal integrity and protects muscle from damage via the LG domain-binding motif of α-DG.

Results

Dystroglycan and Integrin Play Different Roles in Skeletal Muscle. Both α-DG and integrin α7β1 are present in skeletal muscle and function as basal lamina receptors. By using lectin affinity chromatography and sucrose gradient fractionation, we showed that DG and integrin α7β1 are biochemically independent (Fig. S1). Two important features of muscular dystrophy are that the muscle produces reduced force and it is more susceptible to lengthening-contraction-induced (LC-induced) damage. We thus examined the roles of the basal lamina receptors (DG and integrins) on force production and force deficit in response to LC-induced muscle injury by measuring the in vitro contractile properties of the extensor digitorum longus (EDL) muscles (22) of *MCK-cre/Dag1*$^{flox/flpx}$ (DG-null), integrin α7-null (α7-null), and wild-type (WT) mice. The specific forces (kN/m^2) produced by the α7-null and DG-null EDL muscles were significantly decreased by 30% and 22%, respectively, compared with those in control muscle (Fig. 1 *A* and *B*). This result indicates that both α7 and DG play important roles in force generation by muscle. To examine whether disruption of α7 and DG renders muscle more susceptible to LC-induced damage, we delivered two 30% stretches to a maximally activated EDL muscle (23) and this stretch protocol resulted in a force deficit (percentage of force loss after the stretch protocol) of ≈10% in WT EDL muscle (Fig. 1 *C* and *D*). The force deficit in the α7-null EDL muscle was not statistically different (Fig. 1*C*). In contrast, the force deficit of DG-null EDL muscle was 42%, which was 3-fold greater than that in the WT muscle (Fig. 1*D*). The excessive force deficit of DG-null muscle compared with α7-null and WT muscle clearly differentiates the fundamental roles of the 2 receptors, and demonstrates that DG plays a critical role in protecting muscle fibers from damage during lengthening contractions.

Dystroglycan Is Involved in Anchoring the Basal Lamina to the Sarcolemma. Because DG and integrin α7β1 are basal lamina receptors in skeletal muscle, we next determined whether the loss of DG or α7 causes any abnormalities in the basal lamina and/or sarcolemma of skeletal muscle. Analysis of the skeletal muscle fiber ultrastructure by electron microscopy revealed that the basal lamina in both WT and α7-null muscle was intact, and that the association between it and the sarcolemma was tight and continuous (Fig. 1 *E* and *F*). Although DG-null muscle also had an intact basal lamina, an obvious separation of the basal lamina from the sarcolemma was frequently observed (Fig. 1*G*). We also analyzed the muscle ultrastructure after downhill treadmill exercise which causes LC-induced muscle injury in vivo. In both WT and α7-null muscles, we did not detect any obvious changes in the basal lamina, sarcolemma, and myofibril structures after the exercise (Fig. S2). However, DG-null muscle fibers showed severe detachment of the basal lamina from the rest of the fiber and disruption of the underlying sarcomere structure after the exercise (Fig. 1*H* and Fig. S3). These data demonstrate that DG-mediated linkage between the basal lamina and the sarcolemma may play a crucial role in the maintenance of the muscle membrane integrity during lengthening contractions.

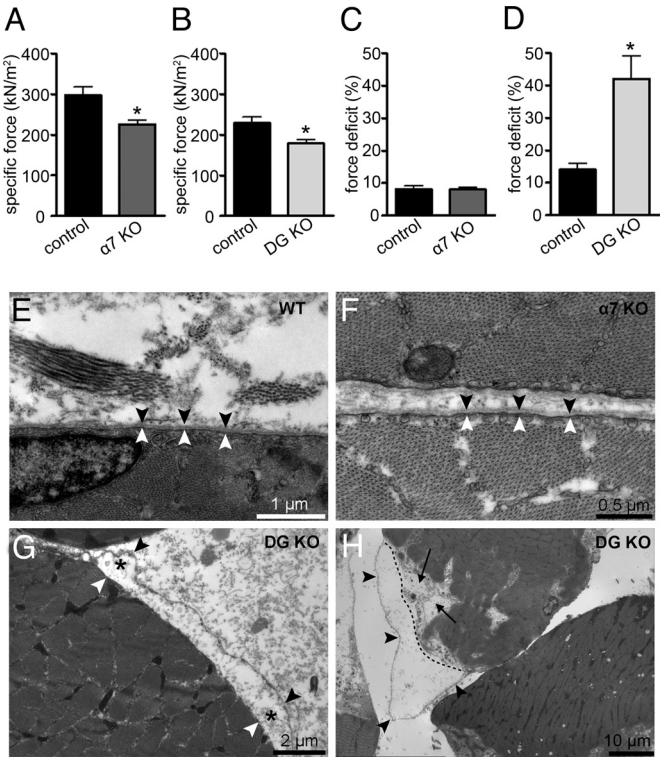

Fig. 1. Contractile and ultrastructural properties of DG- and α7-deficient skeletal muscle. (*A–D*) Specific force (*A* and *B*) and force deficit (*C* and *D*) after 2 lengthening contractions of the EDL muscle from α7-null (α7 KO) and DG-null (DG KO) mice were compared to those for littermate controls. (*, $P < 0.05$.) All data are presented as the mean ± SD. (*E–G*) Ultrastructure of quadriceps muscle from 5-week-old control (*E*), integrin α7-null (*F*), and DG-null (*G*) mice in the absence of exercise. (*H*) Ultrastructure of exercised quadriceps muscle from DG-null mice immediately after downhill treadmill running. Black arrowheads, basal lamina; white arrowhead, sarcolemma; black asterisk, site of separation of the sarcolemma and the basal lamina; dashed line, outline of the disrupted sarcolemma; black arrow, disruption of sarcomere structure.

Severe Muscular Dystrophy in DG/α7 Double Mutant Mice. Integrin and the dystrophin–glycoprotein complex (DGC) show complementary expression patterns in skeletal muscle. Integrin primarily functions at the myotendinous junctions in skeletal muscle whereas DGC functions at both the myotendinous junctions and lateral basal lamina association (24). To further examine the functional complement of integrin and DG, we generated the DG/α7 double mutant (DKO) mice by crossing DG-null and α7-null mice. Loss of both DG and α7 in quadriceps muscle of the DKO mice was confirmed by immunofluorescence and Western blotting analysis (Fig. S4). At birth, the DKO mice were indistinguishable from the littermates, but at ≈4 weeks of age the DKO mice were smaller than their littermates, and they died at ≈6–8 weeks of age. Therefore, we analyzed the DKO mice and the control littermates at 5 weeks of age. DG-null and α7-null mice were indistinguishable from WT mice at this age, whereas the body mass of the DKO mice were about half the mass of littermates (Table S1). We also observed widespread decreases of muscle mass in DKO mice (Table S1). In open field activity assays, the total distance that the DKO mice traveled within 12 h was significantly less than those traveled by either single mutant

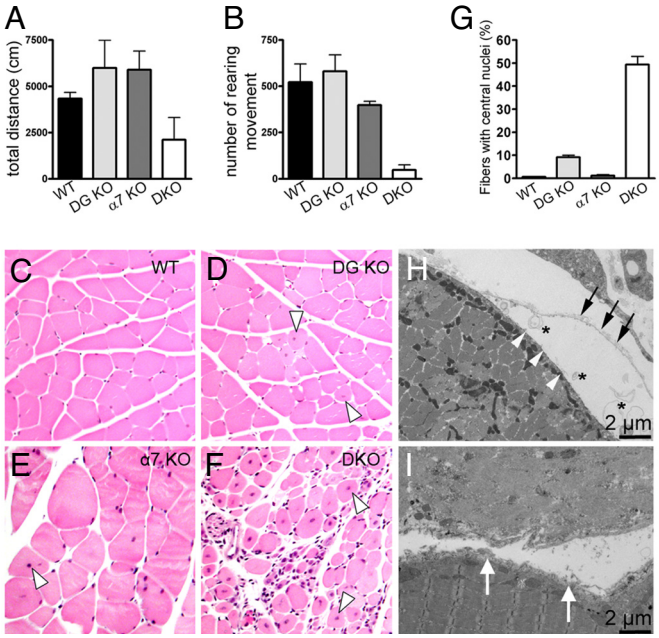

Fig. 2. Severe muscular dystrophy in DG/α7 DKO mice. (*A*) Total distance that the mice traveled within 12 h in open field activity cages. (*B*) Vertical movement activity. Vertical movement activity was represented as the number of rearing movements. DKO significantly impaired vertical movement compared with littermates ($P < 0.01$). The values in all data are averages from 3–7 mice of each group: WT ($n = 7$), DG-null ($n = 6$), α7-null ($n = 4$), and DKO ($n = 3$). (*C–F*) H&E staining of quadriceps sections. Severe pathological changes are observed in DKO section, including variations in fiber size, centrally located nuclei, and infiltration of inflammatory cells. White triangles, centrally nucleated cells. (*G*) Central nucleation is represented as the percentage of total nucleated fibers with centrally located nuclei. (*H* and *I*) Separation of the basal lamina from the sarcolemma (*H*) and loss of the basal lamina structure (*I*) in quadriceps muscles from DKO observed under electron microscopy. White arrowhead, sarcolemma; asterisk, separation of the basal lamina and the sarcolemma; black arrow, detached basal lamina; white arrow, disrupted basal lamina.

(Fig. 2*A*). In addition, the DKO mice showed a dramatic reduction in rearing activity, indicative of severe impairment in hind limb muscle function (Fig. 2*B*). Histological examination of quadriceps at 5 weeks of age revealed more severe hallmarks of muscular dystrophy in DKO mice than DG-null and α7-null mice, characterized by myonecrosis, central nucleation, and variation of fiber size with many small atrophic fibers (Fig. 2 *C–F*). Moreover, infiltration of mononuclear cells was observed in the DKO skeletal muscle. At 5 weeks of age the DKO diaphragm also showed dystrophic pathology similar to the quadriceps muscle. Quantification of the number of muscle cells with central nucleation showed increases in muscle fiber regeneration in DKO compared with DG-null mice (Fig. 2*G*). No significant increase in central nucleation was observed in α7-null mice, which is consistent with the very mild phenotype in young α7-null mice. These data indicate more frequent, on-going muscle degeneration/regeneration in the DKO muscle than each of the single mutant controls. In DKO fibers, in addition to separation of the basal lamina and the sarcolemma (Fig. 2*H*), complete loss of the basal lamina structure was observed (Fig. 2*I*). To distinguish these changes from myonecrosis, disruption of the basal lamina structure was seen adjacent to normal sarcomere structure (Fig. 2*I*, lower fiber). Taken together, these data indicate that both DG and integrin α7 play essential roles in force generation and myofiber–basal lamina association.

***Large*^{myd} Muscle Maintains an Intact DGC but Is Highly Susceptible to the LC-Induced Force Loss.** Our data so far showed that both basal lamina receptors DG and α7 are important for normal skeletal muscle function, but differently from α7, DG is required for maintaining the tight association between the sarcolemma and the basal lamina, which appears to be critical for protecting the muscle against LC-induced muscle injury. However, the DG-null muscle lacks both α-DG and β-DG and thus it is possible that the increased susceptibility to LC-induced injury is caused by the loss of any intracellular connection mediated by β-DG. To dissect out the contribution of the extracellular α-DG in the pathogenesis, we then used *Large*^{myd} mice, the animal model for secondary dystroglycanopathy, which carries an intragenic deletion of exons 4–7 in the *Large* gene, rendering α-DG not properly glycosylated (25). The hypoglycosylated α-DG in *Large*^{myd} muscle lacks the important motif for binding the LG domains of many basal lamina proteins such as laminin, neurexin, agrin (14), and perlecan (26).

To examine whether the muscle with a glycosylation defect in α-DG is susceptible to LC-induced injury, we measured the contractile properties of, and force deficits in, the EDL muscles of *Large*^{myd} mice. The mass of the *Large*^{myd} EDL muscle did not differ from that of the control mice (Fig. 3*A*), but the maximum force generated by *Large*^{myd} EDL muscle was 30% lower than in WT EDL muscle (Fig. 3*B*). Similarly, the specific force (kN/m^2) of *Large*^{myd} muscle was decreased by 33% compared with that of WT control muscle (Fig. 3*C*). These data suggest that fully glycosylated α-DG plays an important role in the ability to transmit contraction force from the sarcomere to the basal lamina, and thus in the ability of muscle to generate force. Moreover, after two 30% stretches of a maximally activated muscle, the force deficits of *Large*^{myd} EDL muscle were 81% (Fig. 3*D*), or 10-fold greater than those in WT EDL muscle. However, by using lectin affinity chromatography and sucrose gradient fractionation, we showed that the muscle of the *Large*^{myd} mouse has an intact DGC (Fig. 3*E*). This is in contrast to other muscular dystrophies involving the DGC, where one primary genetic defect leads to disruption of the entire DGC, as assessed by using the same assay (27, 28). This finding indicates that it is not the loss of the entire DGC, but rather the disrupted linkage between the sarcolemma and the basal lamina (due to disrupted glycosylation of α-DG) (Fig. S5) that is responsible for the high susceptibility to LC-induced muscle injury in secondary dystroglycanopathies.

Electron microscopy analysis of quadriceps muscles from *Large*^{myd} mice also showed large separation between the basal lamina and the sarcolemma (Fig. 3 *F* and *G*). Such separation was also observed in muscles from dystroglycanopathy patients examined (29). Thus, detachment of the basal lamina from the sarcolemma appears to be a common feature for muscular dystrophies caused by DG dysfunction or deficiency, and is likely due to the absence of an interaction between DG and LG domain-containing extracellular matrix proteins such as laminin, agrin, and perlecan.

Dystroglycan Deficiency Compromises Sarcolemma Integrity. Taken together, the large force deficit following lengthening contractions (Figs. 1 and 3), the basal lamina detachment (Figs. 1–3), and the rise in serum creatine kinase activity (30) suggest that muscle is unusually susceptible to LC-induced muscle injury in the absence of functional DG, even when an intact DGC is present. This prompts us to hypothesize that the increased susceptibility in this context is due to compromised transmission of high tensile strength (5, 6) from the basal lamina to the sarcolemma, and that this decreases sarcolemma integrity. To test this, we developed an in situ membrane damage assay (Fig. 4*A*). This assay uses intact muscle fibers in situ, and thus leaves the relationship between the muscle membrane and its basal lamina intact. In this assay, muscle fibers are irradiated with a mode-locked Ti-Sapphire infrared (IR) laser at 880 nm wavelength to induce the loss of membrane integrity at a precise

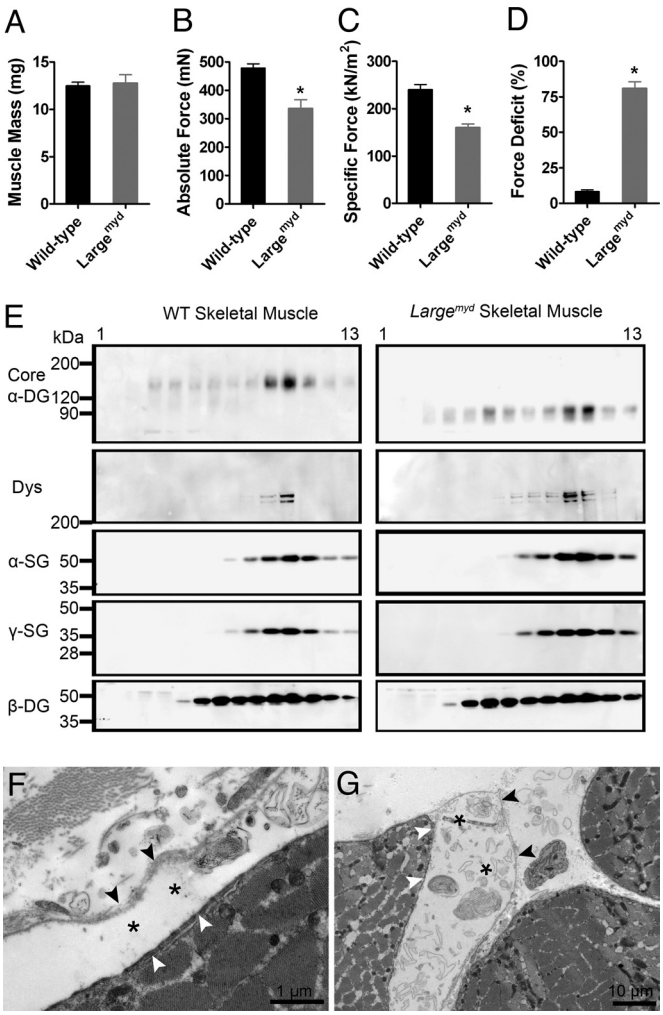

Fig. 3. Characterization of the contractile properties and the DGC structure in the *Large*^{myd} muscle. (*A–C*) EDL muscle mass (*A*), maximum force (*B*), and specific force (*C*) before subjection to the lengthening-contraction protocol. (*D*) Force deficits following the lengthening-contraction protocol, as measured for EDL muscles in vitro from C57BL/6 ($n = 6$) and *Large*^{myd} ($n = 6$) mice. (*, $P < 0.05$.) All data are presented as the mean ± SEM. (*E*) Solubilized C57BL/6 and *Large*^{myd} skeletal muscle were enriched for DGC by wheat germ agglutinin (WGA) affinity chromatography and separated on 10–30% sucrose gradients. Gradient fractions (1, top; 13, bottom) were blotted with antibodies against core α-DG, dystrophin (Dys), α-sarcoglycan (SG), γ-SG, and β-DG. (*F* and *G*) Ultrastructural analysis of quadriceps muscles from *Large*^{myd} mice were observed under electron microscopy. Black arrowhead, basal lamina; white arrowhead, sarcolemma; asterisk, dissociation of basal lamina and sarcolemma.

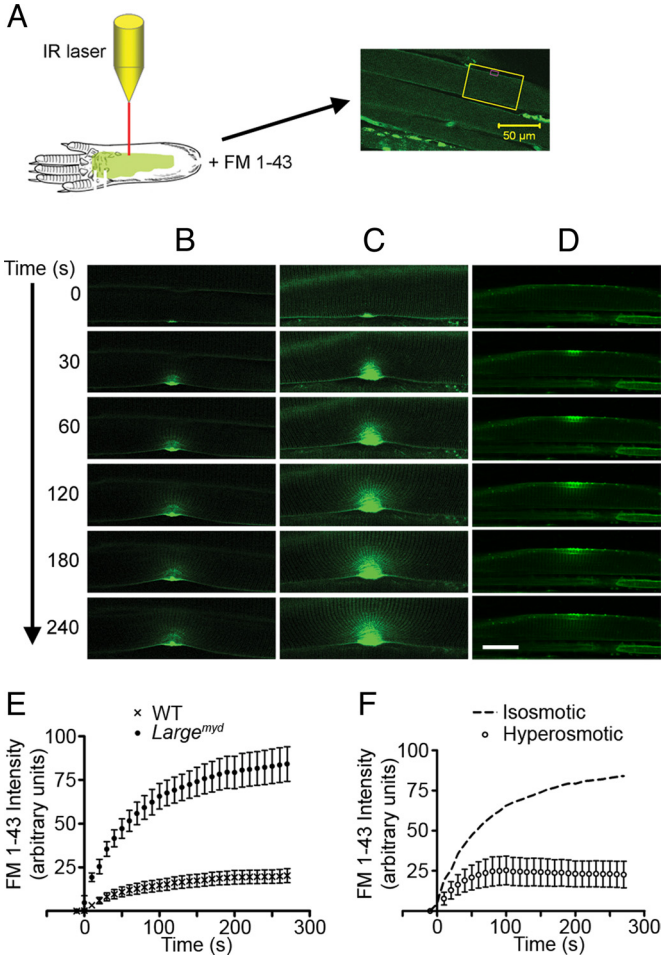

Fig. 4. Membrane damage assay on WT and *Large*^{myd} skeletal muscle. (*A*) Schematics of the in situ membrane damage assay. (*B–D*) Representative examples of time-lapsed images of membrane damage assay performed on C57BL/6 (*B*) and *Large*^{myd} skeletal muscle fibers in regular Tyrode buffer (*C*), or in a hyperosmotic buffer (*D*). (Scale bar: 20 μm.) (*E*) Plot of FM 1-43 fluorescence intensity against time in WT ($n = 7$) and *Large*^{myd} ($n = 8$) muscle fibers. (*F*) Plot of FM 1-43 fluorescence intensity against time in *Large*^{myd} ($n = 5$) muscle fibers in the hyperosmotic buffer. Dashed curve represents membrane damage data in *Large*^{myd} muscle in regular Tyrode buffer (isosmotic), from the experiment whose results are depicted in *E*. All data are presented as mean ± SEM.

region of the sarcolemma in the presence of FM 1-43, a membrane-impermeant fluorescent dye. We found that following irradiation, the FM 1-43 fluorescence concentrated near the laser-irradiated area, and that when the membrane integrity were restored, the increase in fluorescence accumulation halted. Accumulation of FM 1-43 fluorescence was limited to a focal region at the site of damage, and was impeded within 2 min in WT (Fig. 4*B*) muscle fibers, indicating that the membrane integrity had been restored. *Large*^{myd} muscle fibers subjected to the same treatment showed substantially greater FM 1-43 fluorescence accumulation (Fig. 4*C* and Movie S1*B*) than those from WT control mice (Fig. 4*B* and Movie S1*A*). The fluorescence intensity in both cases was plotted vs. the time postdamage (Fig. 4*E*) and fitted with a 1-phase exponential association equation. The maximum fluorescence intensity postirradiation based on the fitted curve was 83.6 ± 2.9, and 20.3 ± 1.4 ($P < 0.001$) for *Large*^{myd} and WT, respectively. In contrast, the apparent rate constants did not differ significantly between the two groups (*Large*^{myd}, 0.016 ± 0.002 s^{-1}; WT, 0.014 ± 0.003 s^{-1}), suggesting that the membrane repair system is unlikely compromised in *Large*^{myd} muscle. Consistent with the DG-null muscle having a normal membrane repair system, the FM 1-43 dye did not diffuse into the entire fiber of *Large*^{myd} muscle as it does in dysferlin-null fibers (31–33). Also, dysferlin immunostaining on the *Large*^{myd} muscle was normal (Fig. S6). Based on these results, we conclude that although the potential of the membrane repair systems seems unaltered in the absence of functional DG, increased loss of the membrane integrity results in more dye entry before the membrane repair machinery can be recruited to repair it.

In further support of this, we reasoned that reducing membrane surface tension should reduce the dye uptake in *Large*^{myd} muscle. We thus performed the membrane damage assay in the *Large*^{myd} muscle in a hyperosmotic buffer (normal physiological

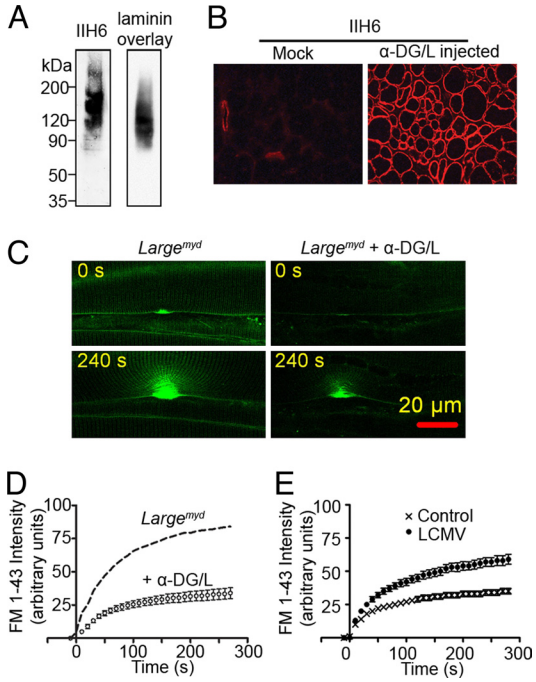

Fig. 5. Effect of α-DG-mediated association of the basal lamina with the sarcolemma on membrane integrity. (*A*) The purified recombinant α-DG reacted with the glycosylated α-DG antibody IIH6 (*Left*) and bound to laminin in the laminin overlay assay (*Right*). (*B*) The *Large*^{myd} muscles injected with recombinant α-DG/L (α-DG/L injected) or saline (Mock) were stained with IIH6 antibody. (*C*) Representative micrographs of membrane damage assay performed on *Large*^{myd} muscle fibers treated with or without recombinant α-DG/L. (*D*) Plot of FM 1-43 fluorescence intensity against time of the in situ membrane damage assay in *Large*^{myd} muscle fibers treated with recombinant α-DG/L ($n = 7$). The dash curve represents mean FM 1-43 fluorescence intensity of the membrane damage assay in *Large*^{myd} muscle from the Fig. 4*E*. (*E*) Plot of FM 1-43 fluorescence intensity against time for the in situ membrane damage assay carried out in C57BL/6 muscle fibers treated with ($n = 9$) or without ($n = 11$) LCMV. All of the data are means ± SEM.

buffer supplemented with 250 mM sucrose). The muscle fiber diameters were decreased in hyperosmotic buffer (Fig. 4*D*), indicating that the muscle fibers shrank. Interestingly, the same level of laser irradiation resulted in very limited dye entry in hyperosmotic buffer (Fig. 4 *D* and *F* and Movie S1*C*). This finding further supports our conclusion that the increased dye entry observed in *Large*^{myd} muscle is due to an increased fragility of the sarcolemma in the absence of α-DG-mediated anchoring of the basal lamina to the sarcolemma.

Consistent with the data showing that integrin α7 does not play a role in stabilizing the sarcolemma, accumulation of FM 1-43 fluorescence in integrin α7-null muscle fibers was similar to that in WT muscle fibers (Fig. S7).

Recombinant Glycosylated α-DG Restores Sarcolemma Integrity in *Large*^{myd} Muscles. Because α-DG is an extracellular protein, we hypothesized that injection of recombinant α-DG extracellularly into *Large*^{myd} muscle would result in the incorporation of α-DG onto the muscle fibers and thus restore membrane integrity. Fully functional, recombinant α-DG was produced in HEK293 cells that were stably cotransfected with α-*dystroglycan* and *Large* expression constructs and purified with lectin affinity chromatography. The purified recombinant α-DG had a smear appearance similar to the native α-DG from skeletal muscle on SDS/PAGE gel, was recognized by the glycosylation epitope antibody IIH6, and bound laminin in the laminin overlay assay (Fig. 5*A*). We then injected the purified α-DG into the tibialis anterior (TA) muscles in *Large*^{myd} mice. Immunofluorescence analysis showed that the recombinant α-DG successfully incorporated onto the sarcolemma (Fig. 5*B*). We also injected the recombinant α-DG into the TA muscles of DG-null mice. However, the IIH6 signal was not increased compared with the noninjected muscle of the same mice (Fig. S8), suggesting that β-DG is required for securing the recombinant α-DG on the sarcolemma. To examine the membrane integrity of the paw muscles from *Large*^{myd} mice injected with recombinant α-DG, we conducted the membrane damage assay on these muscle fibers. Compared to the noninjected *Large*^{myd} muscle fibers, the α-DG injected muscle fibers showed a great reduction in the dye entry after damage (Fig. 5 *C* and *D*). These data suggest that the recombinant α-DG can bind to both the sarcolemma and the basal lamina and thereby restore normal muscle membrane integrity in *Large*^{myd} mouse.

Competitive LCMV-Induced Dissociation of the Basal Lamina from Dystroglycan Increases Membrane Fragility. Previously, α-DG was identified as a major receptor for the Old World arenavirus LCMV, as well as for the human pathogenic LFV (16). LCMV is able to compete with LG domain-containing basal lamina proteins for receptor binding, but unlike basal lamina proteins, the interaction between the virus and α-DG is not dependent on divalent cations (34). This characteristic allows us to examine whether dissociation of basal lamina from α-DG in WT muscle in response to LCMV exposure increases susceptibility of the membrane to injury. We incubated a WT mouse hind-paw preparation in Ca^{2+}/Mg^{2+}-free Tyrode buffer, with or without UV-inactivated LCMV clone-13 (10^7 pfu/mL before UV inactivation). This virus preparation can bind to α-DG but is not infectious. The muscle preparation was then washed in normal Tyrode buffer containing Ca^{2+}/Mg^{2+} and warmed to 37 °C before the membrane damage assay was performed. Pretreatment of the muscle fibers with LCMV significantly increased the magnitude of FM 1-43 dye uptake (Fig. 5*E* and Movies S2 *A* and *B*). This result further supports our overall hypothesis that tight association of the basal lamina with the muscle sarcolemma through fully glycosylated α-DG strengthens the sarcolemma integrity.

Discussion

Over the course of evolution, cells have developed several strategies to maintain or recover the integrity of the plasma membrane. Previous studies have shown that animal cells can survive limited membrane insults due to an active membrane repair mechanism that involves Ca^{2+}-regulated exocytosis (32, 35). In the present study, we have shown a previously uncharacterized mechanism that the skeletal muscle cells use to strengthen the sarcolemma integrity, anchoring the sarcolemma to the basal lamina via laminin G domain-binding motif on α-DG.

Secondary dystroglycanopathies are a group of severe muscular dystrophies in which the underlying genetic defects are the genes that encode proteins known, or thought, to be important for the posttranslational processing of DG (36). In contrast to the muscle fibers in other DGC-related muscular dystrophies, those in secondary dystroglycanopathies retain an intact DGC (14) but are nevertheless highly susceptible to contraction-induced injury (Fig. 3). This observation was our motivation for investigating the exact cause of membrane susceptibility to injury in the muscles of secondary dystroglycanopathies. In the study presented here, we showed that hypoglycosylated DG fails to anchor the basal lamina to the sarcolemma, thereby rendering the muscle prone to damage. We have shown that following laser-induced membrane damage, *Large*^{myd} muscle fibers take up more FM 1-43 dye than WT muscle fibers. This result indicates that loss of functional α-DG directly renders the sarcolemma more

prone to damage. This finding is further supported by the observations that (*i*) reducing membrane tension by incubating the muscle in a buffer with high osmolarity greatly reduced the dye uptake in *Large*^{myd} muscle fibers; (*ii*) injection of recombinant glycosylated α-DG normalized the dye uptake in *Large*^{myd} muscle fibers; and (*iii*) displacing the basal lamina from the sarcolemma in WT muscle fibers by adding inactivated LCMV significantly increased dye uptake.

Interestingly, the type of protection we report here seems to be conserved in other species such as yeast. Yeast and other fungi are surrounded by a cell wall, an essential structure that is required to maintain cell shape and integrity under stress. Several glycosylated proteins—including members of the cell wall integrity and stress response component (WSC) family (Wsc1p to Wsc4p), Mid2p and the Mid2p homologue Mtl1p—are known to play major roles in sensing the cell wall changes in yeast (37). They share a common structural organization: an extracellular domain, a transmembrane segment, and a short cytoplasmic tail. The extracellular domains of these proteins are highly O- and N-glycosylated, and both types of glycosylation are essential for their functionality (37). This structure–function relationship is similar to that of DG in animals. In light of these similarities, our study suggests that molecular transmission of the high tensile strength from an extracellular matrix to the plasma membrane is a general strategy used by cells to maintain the stability of their plasma membrane.

Although both DG and integrin family members function as receptors for basal lamina proteins, our data clearly differentiate their primary roles in muscle fibers. The α7-null muscle fibers neither took up more dye in response to laser-induced membrane damage nor were more susceptible to LC-induced muscle injury than their WT counterparts. Furthermore, we did not observe a separation of the basal lamina from the sarcolemma as in the *Large*^{myd} and DG-null muscle fibers. The molecular basis underlying the difference between DG and integrin is unclear, but this may be related to their different binding affinities for basal lamina proteins. Integrin α7β1 was reported to bind laminin only, but α-DG has been shown to bind a variety of basal lamina proteins containing the LG domains, such as laminin (9, 38), perlecan (11), and agrin (12). In addition, considerable data showed that integrin α7β1 primarily functions at the myotendinous junctions (20, 24, 39, 40) and thus, by its localization, its effects on lateral membrane stability may be minimal.

Collectively, our data suggest that the basal lamina is tightly associated with the sarcolemma through DG binding to the LG domains of the basal lamina proteins of skeletal muscle. Lengthening contractions cause an increase in membrane tension on the sarcolemma, which can lead to small tears in the membrane. The membrane repair mechanism subsequently reseals these membrane tears and thus restores the membrane integrity of myofibers. In DG-null skeletal muscle, molecular linkage of the sarcolemma to the basal lamina is greatly reduced, and the tight association of the sarcolemma with the basal lamina is lost (Fig. 6). Small membrane tears caused by lengthening contractions expand, leading to the loss of a large segment of the membrane, and eventually to muscle-cell necrosis. Thus, the presence of DG allows the basal lamina [which has a much higher tensile strength than the lipid bilayer (4, 5)] to prevent the sarcolemma from rupturing. This mechanism appears to be a basic principle of fracture mechanics of thin layers or membranes: The fracture instability of a crack will not lead to further breakage if the yield stress strength of the adhesive is high enough (41). This principle of fracture mechanics can be illustrated with a balloon which fails to pop when the site of puncture is reinforced by a piece of adhesive tape (Movie S3). The inflated balloon represents the sarcolemma of a muscle fiber undergoing a lengthening contraction, the adhesive represents α-DG and the tape represents

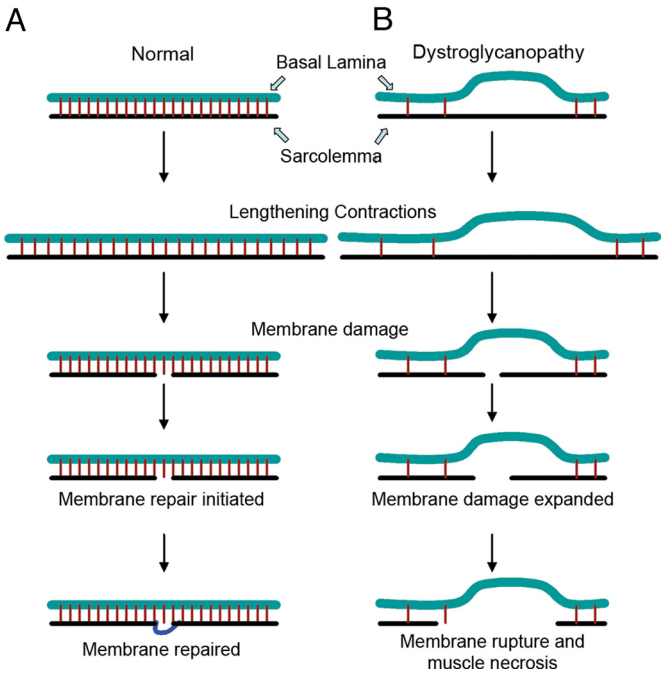

Fig. 6. A proposed mechanism for the basal-lamina-mediated prevention of membrane damage during lengthening contractions. (*A*) In normal skeletal muscle, the sarcolemma is tightly associated with the basal lamina. Lengthening contractions cause an increase in tension within the sarcolemma, which can lead to small membrane tears. The dysferlin-mediated membrane repair mechanism subsequently reseals the membrane and maintains membrane integrity. (*B*) In DG-null skeletal muscle, the tight association of the sarcolemma with the basal lamina is lost, and thus membrane tears that developed during lengthening contractions rapidly expand, leading to the loss of a large segment of the sarcolemma.

the basal lamina. The adhesive links the balloon to the tape just as α-DG links the sarcolemma to the basal lamina. When the tape is applied to the balloon, one can insert the needle (representative of a membrane tear) through the tape and the balloon without rupturing the balloon. In this case the presence of the tape, which has a much higher tensile strength than the balloon, prevents rapid crack advance and thus rupture. In the absence of the tape or adhesive, the balloon does not have enough stress strength, thus the needle ruptures the balloon. Therefore, DG-dependent tight physical attachment of the basal lamina to the sarcolemma is important for transmission of the basal lamina's structural strength to the sarcolemma to provide resistance to mechanical stress. Our findings support the idea that reinforcement of the basal lamina–sarcolemma attachment is a basic cellular mechanism that allows cell survival in tissues subjected to mechanical stress.

Materials and Methods

For details of mice, antibodies, reagents, and analysis, see *SI Materials and Methods*.

Measurement of Contractile Properties and Analysis of Muscle Membrane Structure. Mice (*Large*^{myd}, MCK-cre/*Dag1*$^{flox/flox}$, integrin α7-null, and WT littermate control) were maintained at The University of Iowa Animal Care Unit in accordance with animal use guidelines. All animal studies were authorized by the Animal Care Use and Review Committee of The University of Iowa. Muscle mass, fiber length, and maximum force were measured on 6 EDL muscles from 6- to 7-month-old aforementioned mice except *Large*^{myd} mice (3–5-month-old were used). Total cross-sectional area (CSA, cm^2) and specific P_o (kN/m^2) were determined (22). The susceptibility of muscles to contraction-induced injury was assessed by 2 lengthening contractions with a strain of 30% of fiber length (23). The differences between the experimental and WT

samples were assessed by a 1-tailed Student's *t* test, with the assumption of 2-sample equal variance. Quadriceps muscles from nonexercised and exercised mice were prepared for examination by electron microscopy or immunofluorescence as described in *SI Materials and Methods*. Lectin affinity chromatography and sucrose gradient fractionation were used to analyze the membrane protein complex integrity (*SI Materials and Methods*).

Membrane Damage Assay. The membrane damage assay was performed on skeletal muscle fibers of 6- to 8-week-old mice from *Large*^{myd}, integrin α7-null, and WT littermate control groups. The whole foot was cut off and the skin was removed. The connective tissues and blood vessels were trimmed off to completely expose the muscle fibers. This preparation was placed in a glass-bottom culture dish filled with Tyrode solution containing 1.8 mM Ca^{2+}. Individual fibers were selected for the assay. Membrane damage was induced in the presence of 2.5 μM FM 1-43 dye (Molecular Probes) with a 2-photon confocal laser-scanning microscope (LSM 510; Zeiss) coupled to a 10-W Argon/Ti:sapphire laser. After we scanned images predamage, a 7.9-μm $\times$ 4.4-μm area of the sarcolemma on the surface of the muscle fiber was irradiated at full power for 1.29 seconds. Fluorescence images were captured at 10-second intervals for 10 min after the initial damage. The fluorescence intensities at the damaged site were semiquantified by using ImageJ software. To test the effect of reduced membrane tension on membrane integrity, the assay was also performed on *Large*^{myd} fibers when placed in a hyperosmotic solution. The effects of the UV-inactivated LCMV clone 13 (10^7 pfu/mL) and recombinant glycosylated α-DG (*SI Materials and Methods*) on membrane integrity in WT and *Large*^{myd} muscle fibers, respectively, were also examined by using this assay.

ACKNOWLEDGMENTS. We thank members of the Campbell laboratory for fruitful discussions and Keith Garringer and Sally Prouty for technical support. We also thank the University of Iowa Roy J. and Lucille A. Carver College of Medicine and Microscope Imaging Facility. This work was supported in part by Paul D. Wellstone Muscular Dystrophy Cooperative Research Center Grant 1U54NS053672, Muscular Dystrophy Association Grant MDA3936 (to K.P.C.), a Muscular Dystrophy Association Development grant (to E.P.R.), Welcome Trust Grant 060549 (to U.M), and U.S. Department of Defense Grant W81XWH-05-1-0079. K.P.C. is an investigator of the Howard Hughes Medical Institute.

1. Davies KE, Nowak KJ (2006) Molecular mechanisms of muscular dystrophies: Old and new players. *Nat Rev Mol Cell Biol* 7:762–773.
2. Durbeej M, Campbell KP (2002) Muscular dystrophies involving the dystrophin-glycoprotein complex: An overview of current mouse models. *Curr Opin Genet Dev* 12:349–361.
3. Meryon E (1852) On granular and fatty degeneration of voluntary muscles. *Med Chir Trans* 35:73–84.
4. Sanes JR (2003) The basement membrane/basal lamina of skeletal muscle. *J Biol Chem* 278:12601–12604.
5. Candiello J, et al. (2007) Biomechanical properties of native basement membranes. *FEBS J* 274:2897–2908.
6. Grounds MD, Sorokin L, White J (2005) Strength at the extracellular matrix-muscle interface. *Scand J Med Sci Sports* 15:381–391.
7. Timpl R, Brown JC (1996) Supramolecular assembly of basement membranes. *Bioessays* 18:123–132.
8. Miner JH, Yurchenco PD (2004) Laminin functions in tissue morphogenesis. *Annu Rev Cell Dev Biol* 20:255–284.
9. Ibraghimov-Beskrovnaya O, et al. (1992) Primary structure of dystrophin-associated glycoproteins linking dystrophin to the extracellular matrix. *Nature* 355:696–702.
10. Burkin DJ, Kaufman SJ (1999) The alpha7beta1 integrin in muscle development and disease. *Cell Tissue Res* 296:183–190.
11. Talts JF, Andac Z, Gohring W, Brancaccio A, Timpl R (1999) Binding of the G domains of laminin alpha1 and alpha2 chains and perlecan to heparin, sulfatides, alpha-dystroglycan and several extracellular matrix proteins. *EMBO J* 18:863–870.
12. Gee SH, Montanaro F, Lindenbaum MH, Carbonetto S (1994) Dystroglycan-alpha, a dystrophin-associated glycoprotein, is a functional agrin receptor. *Cell* 77:675–686.
13. Michele DE, Campbell KP (2003) Dystrophin-glycoprotein complex: Post-translational processing and dystroglycan function. *J Biol Chem* 278:15457–15460.
14. Michele DE, et al. (2002) Post-translational disruption of dystroglycan-ligand interactions in congenital muscular dystrophies. *Nature* 418:417–422.
15. Barresi R, et al. (2004) LARGE can functionally bypass alpha-dystroglycan glycosylation defects in distinct congenital muscular dystrophies. *Nat Med* 10:696–703.
16. Cao W, et al. (1998) Identification of alpha-dystroglycan as a receptor for lymphocytic choriomeningitis virus and Lassa fever virus. *Science* 282:2079–2081.
17. Rambukkana A, et al. (1998) Role of alpha-dystroglycan as a Schwann cell receptor for *Mycobacterium leprae*. *Science* 282:2076–2079.
18. Williamson RA, et al. (1997) Dystroglycan is essential for early embryonic development: Disruption of Reichert's membrane in Dag1-null mice. *Hum Mol Genet* 6:831–841.
19. Mayer U (2003) Integrins: Redundant or important players in skeletal muscle? *J Biol Chem* 278:14587–14590.
20. Mayer U, et al. (1997) Absence of integrin alpha 7 causes a novel form of muscular dystrophy. *Nat Genet* 17:318–323.
21. Hayashi YK, et al. (1998) Mutations in the integrin alpha7 gene cause congenital myopathy. *Nat Genet* 19:94–97.
22. Brooks SV, Faulkner JA (1988) Contractile properties of skeletal muscles from young, adult and aged mice. *J Physiol* 404:71–82.
23. Dellorusso C, Crawford RW, Chamberlain JS, Brooks SV (2001) Tibialis anterior muscles in mdx mice are highly susceptible to contraction-induced injury. *J Muscle Res Cell Motil* 22:467–475.
24. Kaariainen M, et al. (2000) Integrin and dystrophin associated adhesion protein complexes during regeneration of shearing-type muscle injury. *Neuromuscul Disord* 10:121–132.
25. Grewal PK, Holzfeind PJ, Bittner RE, Hewitt JE (2001) Mutant glycosyltransferase and altered glycosylation of alpha-dystroglycan in the myodystrophy mouse. *Nat Genet* 28:151–154.
26. Kanagawa M, et al. (2005) Disruption of perlecan binding and matrix assembly by post-translational or genetic disruption of dystroglycan function. *FEBS Lett* 579:4792–4796.
27. Durbeej M, et al. (2000) Disruption of the beta-sarcoglycan gene reveals pathogenetic complexity of limb–girdle muscular dystrophy type 2E. *Mol Cell* 5:141–151.
28. Beedle AM, Nienaber PM, Campbell KP (2007) Fukutin-related protein associates with the sarcolemmal dystrophin–glycoprotein complex. *J Biol Chem* 282:16713–16717.
29. Sabatelli P et al. (2003) Extracellular matrix and nuclear abnormalities in skeletal muscle of a patient with Walker–Warburg syndrome caused by POMT1 mutation. *Biochim Biophys Acta* 1638:57–62.
30. Cohn RD, et al. (2002) Disruption of DAG1 in differentiated skeletal muscle reveals a role for dystroglycan in muscle regeneration. *Cell* 110:639–648.
31. Bansal D, et al. (2003) Defective membrane repair in dysferlin-deficient muscular dystrophy. *Nature* 423:168–172.
32. Han R, Campbell KP (2007) Dysferlin and muscle membrane repair. *Curr Opin Cell Biol* 19:409–416.
33. Han R, et al. (2007) Dysferlin-mediated membrane repair protects the heart from stress-induced left ventricular injury. *J Clin Invest* 117:1805–1813.
34. Kunz S, Sevilla N, McGavern DB, Campbell KP, Oldstone MB (2001) Molecular analysis of the interaction of LCMV with its cellular receptor α-dystroglycan. *J Cell Biol* 155:301–310.
35. McNeil PL, Kirchhausen T (2005) An emergency response team for membrane repair. *Nat Rev* Mol Cell Biol 6:499–505.
36. Muntoni F, Torelli S, Brockington M (2008) Muscular dystrophies due to glycosylation defects. *Neurotherapeutics* 5:627–632.
37. Levin DE (2005) Cell wall integrity signaling in *Saccharomyces cerevisiae*. *Microbiol Mol Biol Rev* 69:262–291.
38. Ervasti JM, Campbell KP (1993) A role for the dystrophin-glycoprotein complex as a transmembrane linker between laminin and actin. *J Cell Biol* 122:809–823.
39. van der Flier A, et al. (1997) Spatial and temporal expression of the beta1D integrin during mouse development. *Dev Dyn* 210:472–486.
40. Miosge N, Klenczar C, Herken R, Willem M, Mayer U (1999) Organization of the myotendinous junction is dependent on the presence of alpha7beta1 integrin. *Lab Invest* 79:1591–1599.
41. Broek D (1986) *Elementary Engineering Fracture Mechanics* (Martinus Nijhoff, Dordrecht, The Netherlands) 4th Ed.

Supporting Information

Han et al. 10.1073/pnas.0906545106

SI Materials and Methods

Mice. Mice with striated-muscle-specific dystroglycan (DG) deficiency (MCK-cre/*Dag1*$^{flox/flox}$) (1) and integrin α7-null (2) mice were described previously. For a direct comparison of DG-deficient and integrin α7-null skeletal muscle in the same mouse line, these 2 mouse lines were crossed to one another. MCK-Cre male mice bearing the floxed *dystroglycan* allele were mated to *integrin* α7 heterozygous females. F1 and F2 offspring were mated to produce F2- and F3-generation mice, respectively. Identification of the mutant mice was performed by PCR genotyping of genomic DNA prepared from mouse tail snips. The *Large*^{myd} colony was originally obtained from Jackson Laboratories. Mice were maintained at The University of Iowa Animal Care Unit in accordance with animal use guidelines. All animal studies were authorized by the Animal Care Use and Review Committee of The University of Iowa. For treadmill exercise, mice ($\approx$5 weeks old) were placed on an endless conveyor-type belt with a shock grid at the end (AccuPacer Treadmill, AccuScan Instruments) and exercised on a down-hill grade at 15 m/min for 20 min. Immediately after the exercise, mice were euthanized and quadriceps muscles were prepared for examination by electron microscopy or immunofluorescence.

Lectin Affinity Chromatography and Sucrose Gradient Fractionation. Total muscle homogenates in TBS (50 mM Tris-Cl pH 7.4, 150 mM NaCl) were solubilized with 1% digitonin. After centrifugation at 140,000 $\times$ *g* for 37 min, solubilized proteins in the supernatant were mixed with wheat germ agglutinin (WGA)-agarose beads (Vector Laboratories) and rotated end-over-end at 4 °C for 2 h. WGA-bound proteins were eluted with TBS containing 0.3 M N-acetyl-D-glucosamine and 0.1% digitonin. The eluant was applied to a 5–30% sucrose gradient and centrifuged at 215,000 $\times$ *g* for 90 min. Fractions (1 mL) were collected from the top of the gradient and analyzed by SDS/PAGE.

Measurement of Contractile Properties. Muscle mass, fiber length, and maximum force were measured on 6 EDL muscles from 6- to 7-month-old *Large*^{myd}, MCK-cre/*Dag1*$^{flox/flox}$, integrin α7-null, and WT littermate control mice. Mice were anesthetized and muscles isolated and stimulated to provide maximum isometric tetanic force (P_o). The susceptibility of muscles to contraction-induced injury was assessed by 2 lengthening contractions with a strain of 30% of fiber length. Total cross-sectional area (CSA, cm^2) and specific P_o (kN/m^2) were determined (3). The differences between the experimental and WT samples were assessed by a 1-tailed Student's *t* test, with the assumption of 2-sample equal variance.

Mouse Behavior Analysis. Locomotor activity was monitored by using Digiscan Animal Activity Monitoring System running Versamax Windows software (Accuscan Instruments). The Versamax Windows software uses a mathematical algorithm to compute total distance traveled (in cm) and rearing number. All mice were tested for 12 h starting from 6PM.

Membrane Damage Assay. The membrane damage assay was performed on skeletal muscle fibers of 6- to 8-week-old mice from *Large*^{myd}, integrin α7-null, and WT littermate control groups. The whole foot was cut off and the skin was removed. The connective tissues and blood vessels were trimmed off to completely expose the muscle fibers. This preparation was placed in a glass-bottom culture dish filled with Tyrode solution containing 1.8 mM Ca^{2+}. Individual fibers were selected for the assay. Regenerating muscle fibers (centrally nucleated or with small diameters) were carefully excluded from the assay. Membrane damage was induced in the presence of 2.5 μM FM 1-43 dye (Molecular Probes) with a 2-photon confocal laser-scanning microscope (LSM 510; Zeiss) coupled to a 10-W Argon/Ti:sapphire laser. After we scanned images predamage, a 7.9-μm x 4.4-μm area of the sarcolemma on the surface of the muscle fiber was irradiated at full power for 1.29 seconds. Fluorescence images were captured at 10-second intervals for 10 min after the initial damage. The fluorescence intensities at the damaged site were semiquantified by using ImageJ software.

Production of Recombinant Glycosylated α-DG. A stable HEK293F cell line (Invitrogen) expressing both of *α-dystroglycan* and *Large* was generated to produce the recombinant α-DG that bound LG domain proteins with high affinity. The recombinant protein was enriched from the SFMII media (Invitrogen) of this cell line by agarose-bound WGA (Vector laboratories).

Injection of Purified Recombinant α-DG into *Large*^{myd} Muscles. Before the injection to *Large*^{myd} mice, the buffer was changed to sterile 0.9% saline by Amicon Ultra (Milipore). The calf, tibial anterior, and paw muscles of *Large*^{myd} mice were injected with 50, 30, and 10 μL of the purified recombinant α-DG (200 μg/mL) or saline, respectively. The muscles were excised 5 days after injection and were analyzed by immunofluorescence staining or membrane damage assay.

Laminin Overlay Assay. Laminin overlay assays were performed on PVDF membranes by using mouse Engelbreth–Hol–Swarm (EHS) laminin as previously described (4). Briefly, PVDF membranes were blocked in laminin-binding buffer (LBB: 10 mM triethanolamine, 140 mM NaCl, 1 mM $MgCl_2$, 1 mM $CaCl_2$, pH 7.6) containing 5% BSA followed by incubation with laminin overnight at 4 °C in LBB. Membranes were washed and incubated with anti-laminin (Sigma) followed by anti-rabbit IgG–HRP. Blots were developed by enhanced chemiluminescence.

LCMV Treatment of WT Muscle. The WT mouse foot preparation was incubated with or without the UV-inactivated LCMV clone 13 (10^7 pfu/mL) in ice-cold Ca^{2+}/Mg^{2+}-free Tyrode solution for 2 h. The preparation was then washed twice with ice-cold normal Ca^{2+}/Mg^{2+}-containing Tyrode solution, and warmed up to 37 °C. The membrane damage assay was then conducted on these samples as described above.

Electron Microscopy. Mice were anesthetized with ketamine (87.5 mg/kg body weight), and a bilateral sternum incision was performed to expose the left atrium. Mice were perfused with PBS and then with 2% paraformaldehyde in PBS. Quadriceps muscle blocks were dissected into pieces (1 mm x 3 mm) and fixed by using Karnowsky's fixative (2.5% glutaraldehyde and 2% paraformaldehyde in 0.1M cacodylate buffer, pH 7.4) for 2 h at 4 °C. Tissue blocks were washed in 0.1 M cacodylate buffer (2 $\times$ 5 min), processed through a 6-hour routine EM processing schedule, and then infiltrated with epon/alardite resin (Electron Microscopy Sciences) on a Leica EM TP automatic tissue processor. Tissues were embedded, oriented longitudinally and transversely, placed in a vacuum-infiltrating oven, and then polymerized at 60 °C for 24 h. Multiple 1-μm thick sections were

stained with 1% toluidine blue in 1% borax. Representative areas were selected, ultrasectioned at 70 nm (silver sections), mounted on 200 mesh athene copper grids, double stained with Reynolds lead citrate and uranyl acetate, and then examined by using a Zeiss 906E electron microscope. Representative digital images were taken by using SIS Keenview camera and software.

1. Cohn RD, et al. (2002) Disruption of DAG1 in differentiated skeletal muscle reveals a role for dystroglycan in muscle regeneration. *Cell* 110:639–648.
2. Mayer U, et al. (1997) Absence of integrin alpha7 causes a novel form of muscular dystrophy. *Nat Genet* 17:318–323.
3. Brooks SV, Faulkner JA (1988) Contractile properties of skeletal muscles from young, adult and aged mice. *J Physiol* 404:71–82.
4. Michele DE, et al. (2002) Post-translational disruption of dystroglycan–ligand interactions in congenital muscular dystrophies. *Nature* 418:417–422.

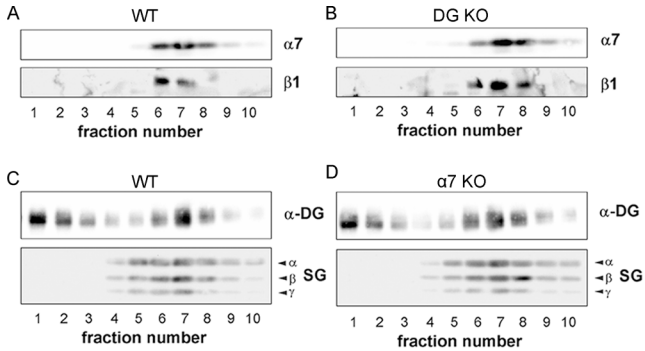

Fig. S1. Characterization of skeletal muscle DG and integrin $\alpha 7$ complexes. (*A–D*) Sucrose gradient fractionation of the DGC and the integrin $\alpha 7$ complex from WT (*A* and *C*), DG-null (*B*), and integrin $\alpha 7$-null (*D*) skeletal muscle solubilized with digitonin. Glycoprotein preparations enriched by WGA-chromatography were fractionated by sucrose gradient centrifugation. Equal volumes of fractions were loaded on an SDS/PAGE gel. The blot generated from this was probed with antibodies against: integrin $\alpha 7$ ($\alpha 7$), integrin $\beta 1$ ($\beta 1$), α-DG (α-DG), α-sarcoglycan (α-SG), β-sarcoglycan (β-SG), and γ-sarcoglycan (γ-SG). Numbers at the bottom of the blot indicate the sucrose gradient fraction number, from top to bottom.

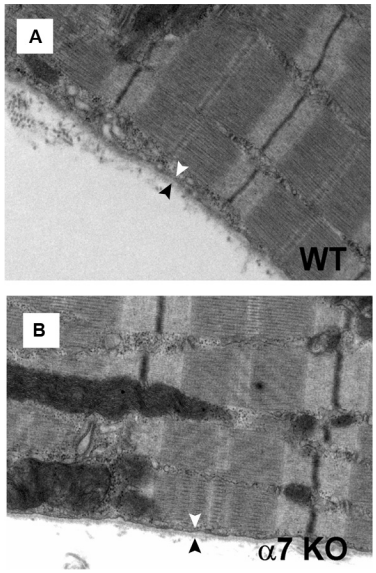

Fig. S2. Ultrastructural analysis of quadriceps muscles from WT (*A*) and α7-null (*B*) mice after exercise. After exercise, there is no detectable abnormality in the basal lamina and the sarcolemma in the muscles from WT and α7-null mice.

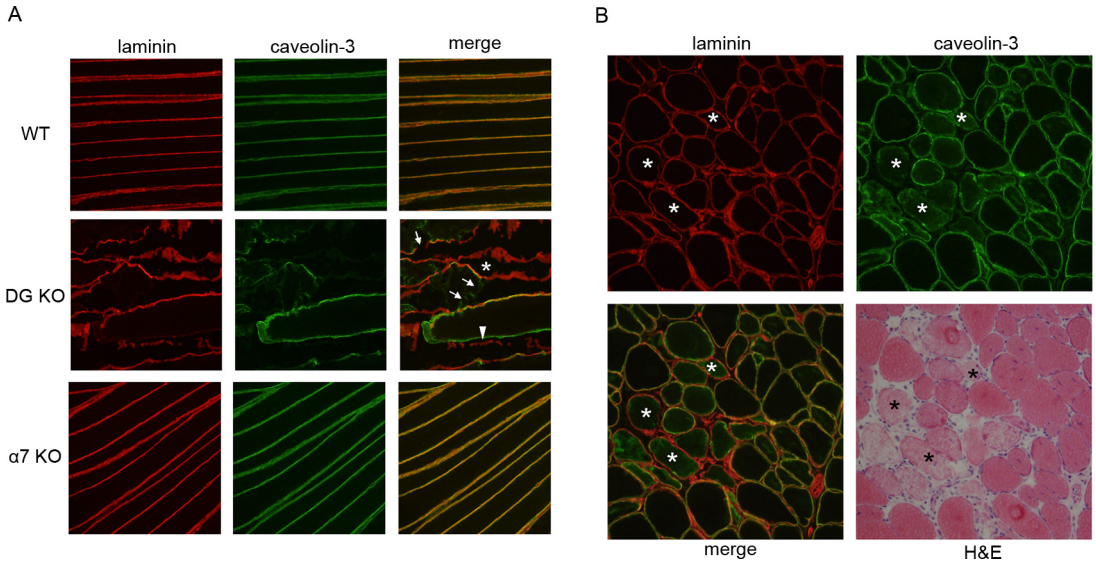

Fig. S3. Exercise-induced dissociation of the basal lamina and the sarcolemma in the DG KO muscle. (*A*) Immunostaining of longitudinal fibers after exercise. Five-week-old mice (WT, DG KO, and α7 KO) were subjected to treadmill-exercise (15° downhill for 20 min). Immediately after the exercise, quadriceps muscles were taken. Longitudinal cryosections were immunostained with laminin and caveolin-3. Arrow, breakage of laminin- or caveolin-3-staining; arrowhead, separation of laminin- and caveolin-3-staining; asterisk, fiber with remaining laminin deposition. (*B*) Acute damage of DG-null muscle after the exercise. Cryosections of DG KO postexercised quadriceps muscle were coimmunostained with laminin and caveolin-3. Serial section was stained with hematoxylin and eosin (H&E). White asterisk, fiber with remaining laminin deposition; black asterisk, necrotic fibers.

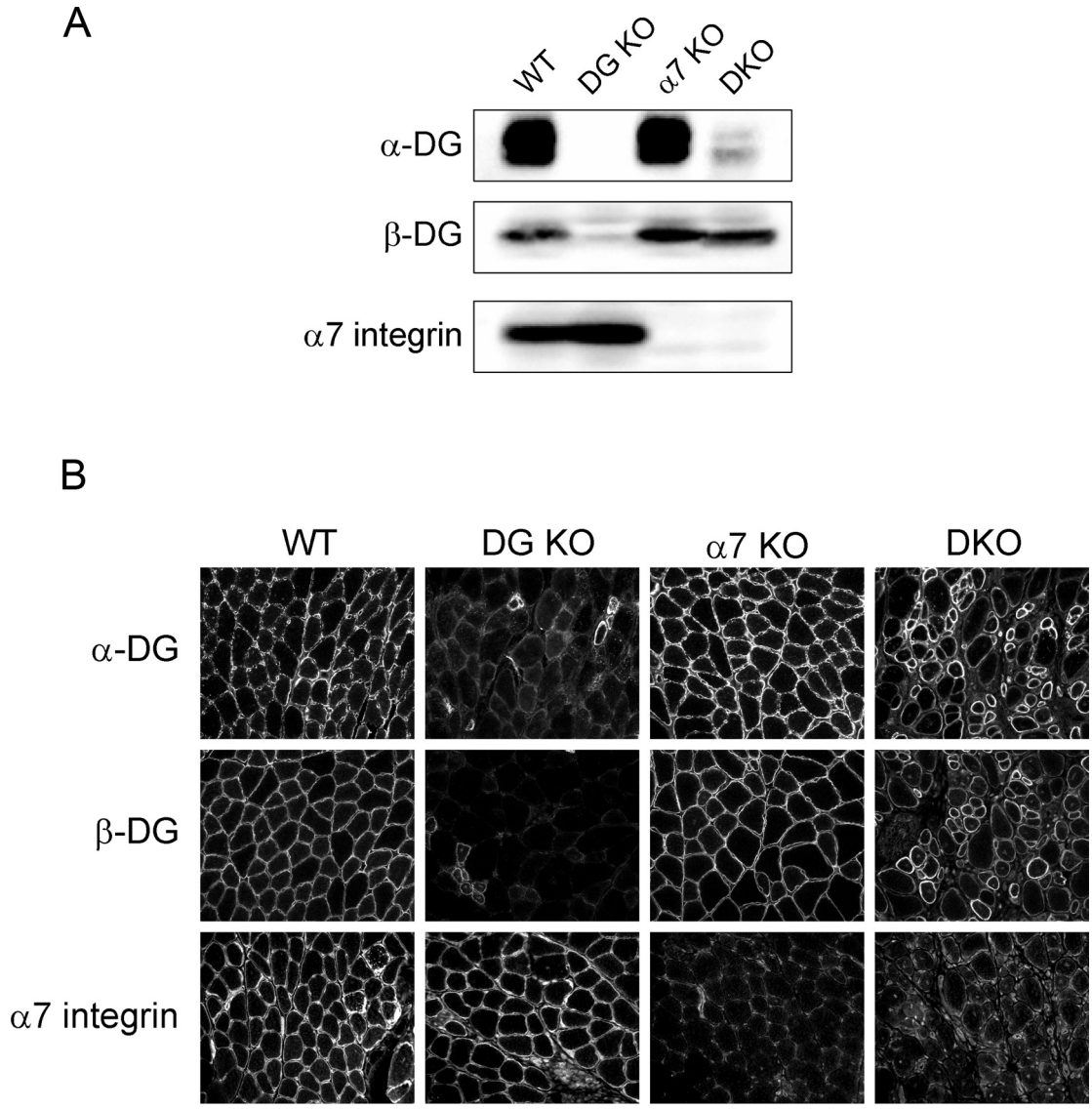

Fig. S4. Disrupted expression of DG and α7 in DG/α7 double mutant (DKO) mice. Western blotting (*A*) and immunofluorescence staining (*B*) analysis showed loss of the DG and α7 expression in DG/α7 DKO muscle. It is of note that the DG expression in DKO is higher than in the DG-null muscle due to the greater regeneration.

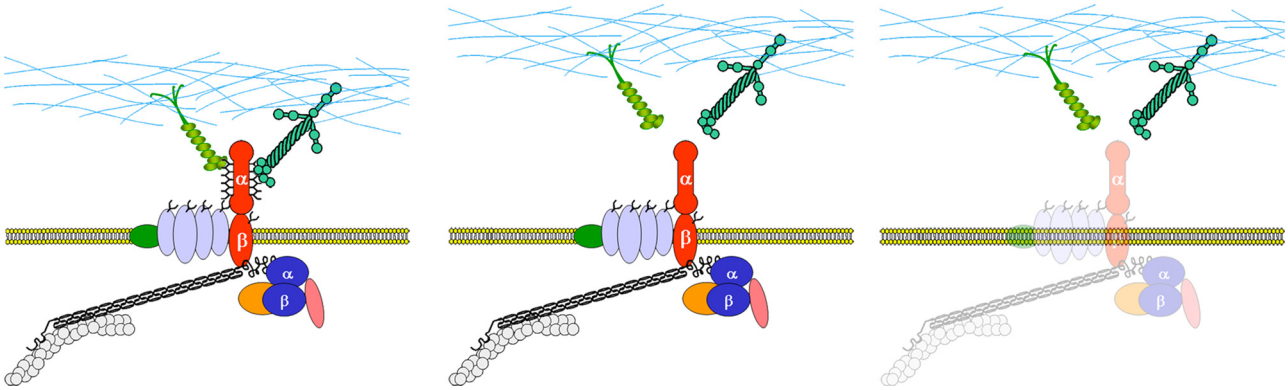

Fig. S5. Schematic models of the DGC in skeletal muscle of different mouse models. (*Left*) WT; (*Center*) *Large*^{myd}; (*Right*) MCK DG-null.

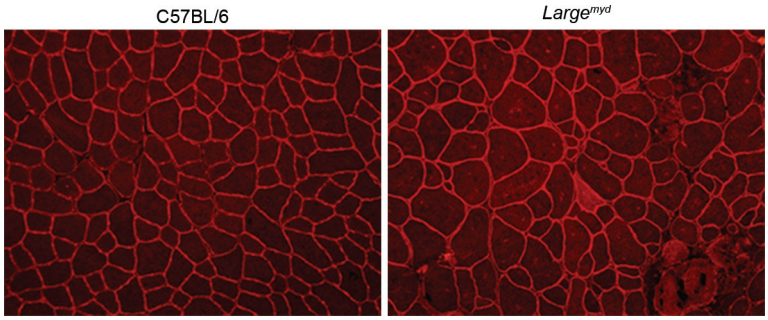

Fig. S6. Immunofluorescence staining of dysferlin in skeletal muscle of *Large*^{myd} mice. Quadriceps muscle sections from WT C57BL/6 and *Large*^{myd} mice were stained with the anti-dysferlin antibody Hamlet.

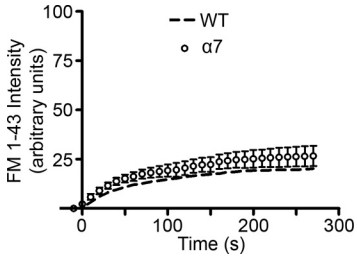

Fig. S7. Damage assay on skeletal muscle of α7-null mice. Plot of FM 1-43 fluorescence intensity against time in integrin α7-null (open square, $n = 5$) muscle fibers. The dashed curve represents mean fluorescence intensity in the membrane damage assay, in wild-type muscle from Fig. 4*E*.

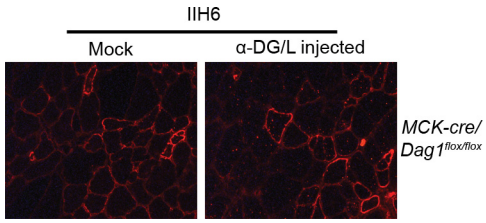

Fig. S8. Stability of recombinant α-DG on the sarcolemma of DG-null muscle fibers DG-null. DG-null muscles injected with recombinant α-DG/L (α-DG/L injected) or saline (Mock) were stained with the glycosylated α-DG antibody (IIH6). Recombinant α-DG failed to stay on the sarcolemma of DG-null muscles, suggesting that β-DG is required for securing the recombinant α-DG on the sarcolemma.

Table S1. Severe loss of body weight and muscle mass in DG/α7 DKO mice

	WT	DG KO	α7 KO	DKO
Body weight, g	23.6 ± 0.4	21.7 ± 3.1	20.8 ± 1.0*	11.2 ± 0.9***
Gastrocnemius, mg	121.4 ± 5.5	125.1 ± 8.3	122.8 ± 8.2	37.5 ± 0.6***
TA, mg	34.9 ± 5.5	33.5 ± 1.5	35.0 ± 1.6	10.1 ± 2.4***
Triceps, mg	72.0 ± 11.6	74.0 ± 21.3	62.3 ± 2.1	22.0 ± 3.2***
Quadriceps, mg	107.4 ± 2.5	126.3 ± 12.5	116.5 ± 17.6	40.6 ± 9.6***
Heart, mg	115.1 ± 14	128.5 ± 34.2	113.9 ± 19.5	71.9 ± 4.8 **
Shin length, cm	2.2 ± 0	2.2 ± 0.1	2.1 ± 0.1	2.1 ± 0.1

*, $P < 0.05$; **, $P < 0.01$; ***, $P < 0.001$; $n = 3$.

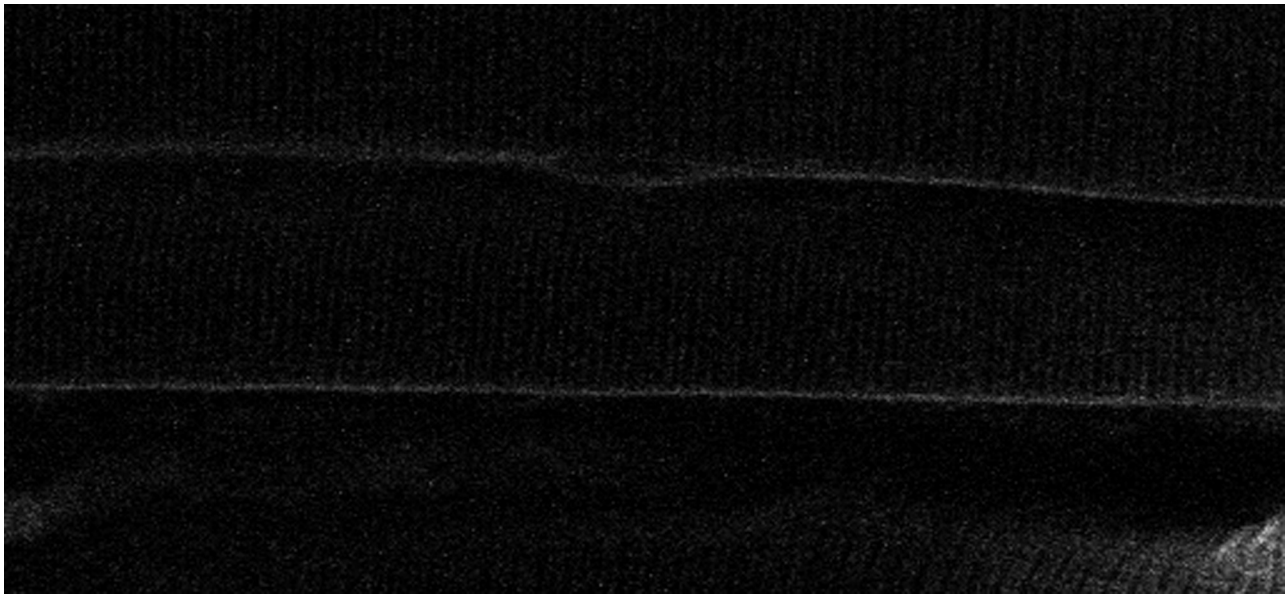

Movie S1*A*. In situ membrane damage assay in C57BL/6 WT muscle.

Movie S1*A* (AVI)

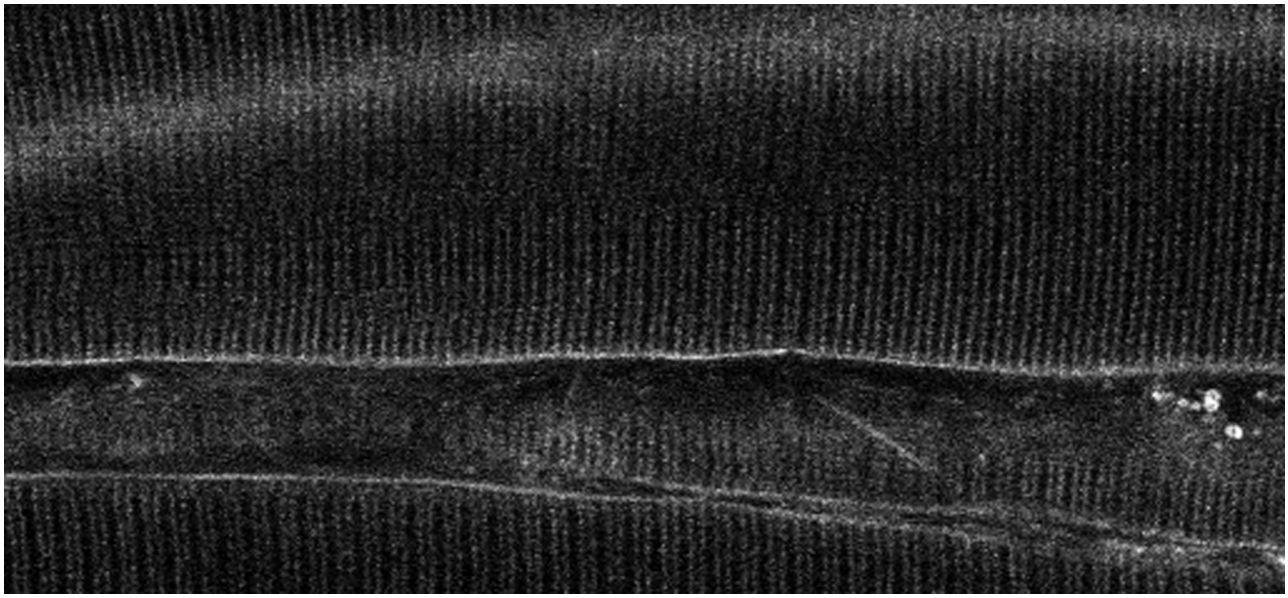

Movie S1*B*. In situ membrane damage assay of *Large*^{myd} muscle in regular buffer.

Movie S1*B* (AVI)

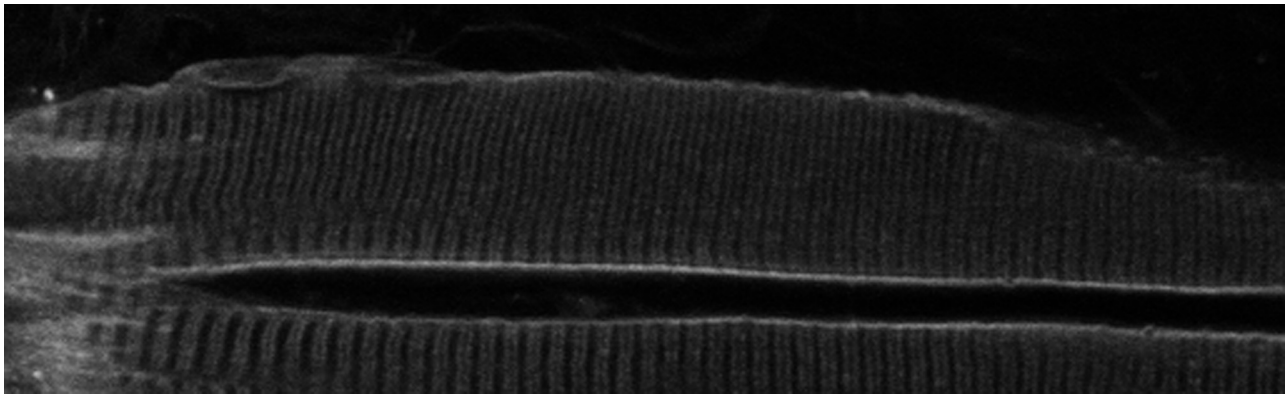

Movie S1C. In situ membrane damage assay of *Large*^{myd} muscle in hyperosmotic buffer.

Movie S1C (AVI)

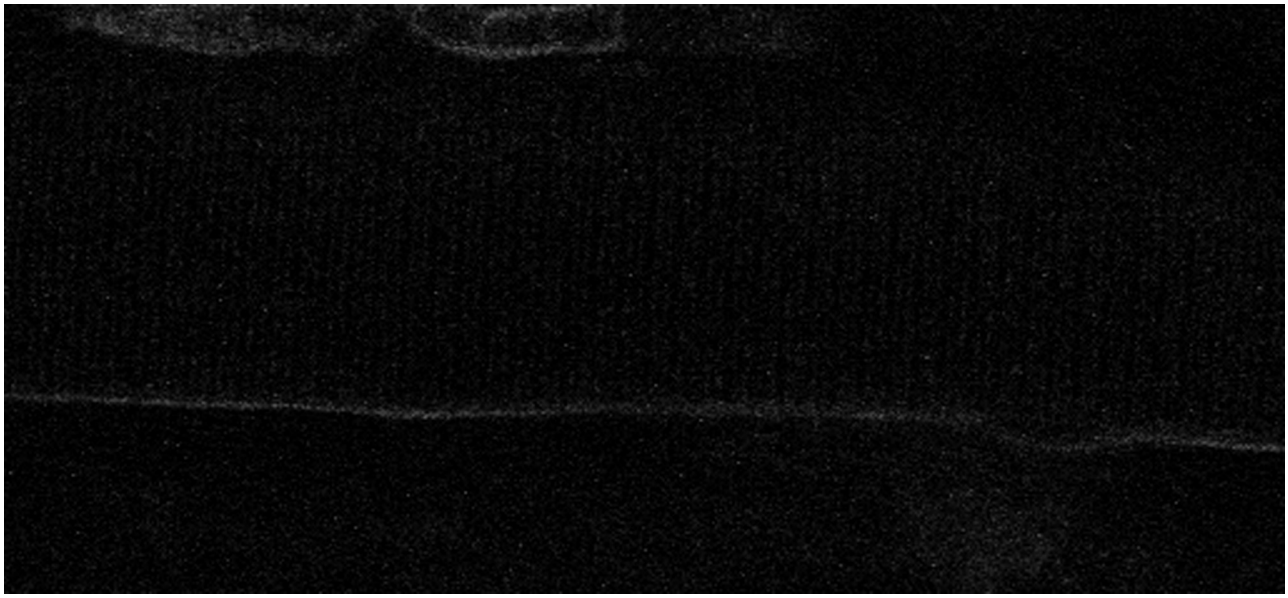

Movie S2*A*. In situ membrane damage assay of C57BL/6 WT muscle subjected to mock treatment.

Movie S2*A* (AVI)

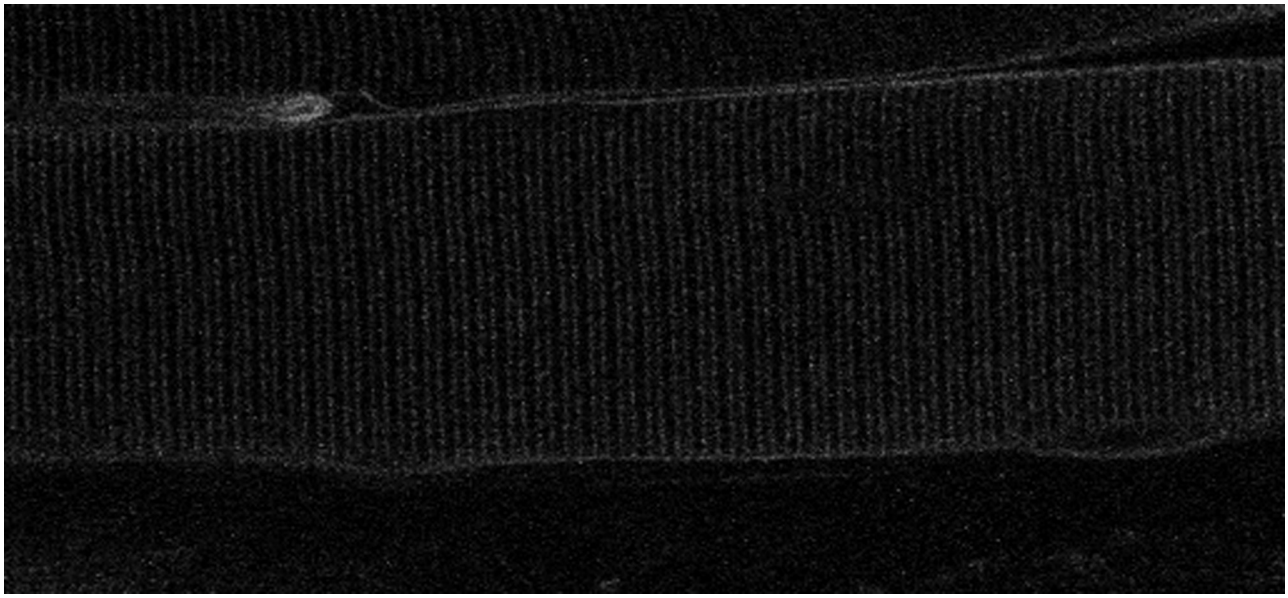

Movie S2*B*. In situ membrane damage assay of C57BL/6 WT muscle subjected to LCMV treatment.

Movie S2*B* (AVI)

Movie S3. Balloon movie.

Movie S3 (WMV)